



## Sand dune dynamics and climate change: A modeling approach

H. Yizhaq,<sup>1</sup> Y. Ashkenazy,<sup>1</sup> and H. Tsoar<sup>2</sup>

Received 19 August 2008; revised 3 November 2008; accepted 12 December 2008; published 24 February 2009.

[1] We provide several examples for the coexistence of active and fixed sand dunes under similar climatic conditions, namely, with respect to wind power and precipitation rate. A model is developed for dune vegetation cover that includes wind power, precipitation rate, and anthropogenic effects, such as grazing and wood gathering. The model reproduces the observed dune's bistability and shows that under intense human pressure and prolonged droughts the fixed dunes may turn active. Moreover, the model shows that the dune reactivation process is almost irreversible, as a fixed dune will become active only under the action of very strong winds and can then return to the fixed state only when wind power decreases far below the levels under which the initial dune maintained its stability. Similar hysteretic behavior of dune mobility is predicted by the model with respect to changing precipitation and human pressure parameters.

**Citation:** Yizhaq, H., Y. Ashkenazy, and H. Tsoar (2009), Sand dune dynamics and climate change: A modeling approach, *J. Geophys. Res.*, 114, F01023, doi:10.1029/2008JF001138.

### 1. Introduction

[2] Among the geomorphological landscapes, sand dunes exhibit interesting forms and dynamics. They cover vast areas of the world's deserts (~20%) [Pye and Tsoar, 1990] (see Figure 1) and usually are associated with unique biological and ecological activity [Danin, 1996]. Dune shapes and dynamics have attracted the attention of scientists interested in grain dynamics, dune formation and dune movement [Bagnold, 1941; Wiggs, 2001; Andreotti *et al.*, 2002; Herrmann, 2006]. Aside from theoretical considerations, dune activity has a more prosaic interest, as in many places around the world (e.g., in northern China, Morocco, and Mauritania), sand dunes are an imminent threat to human property [Dong *et al.*, 2005]. Sand dunes may be fixed, active or partially active, mainly as a function of wind power and vegetation cover. Thus, ongoing climatic changes may turn some currently fixed dunes into active ones and vice versa [Muhs and Maat, 1993; Thomas *et al.*, 2005; Alexander, 2007].

[3] Geomorphologists usually quantify dune mobility in terms of mobility indexes [Lancaster, 1997]. These are usually based on parameters such as wind power, precipitation rate and potential evapotranspiration. According to conventional beliefs, dunes in the same geographical area can be active, fixed or partially active dependent on changing climatological conditions that determine mobility

indexes [Knight *et al.*, 2004]. However, it was recently shown that active and fixed dunes may coexist under similar climatic conditions [Muhs and Maat, 1993; Tsoar, 2005; Yizhaq *et al.*, 2007; Arens *et al.*, 2007]. This fact raises questions about the validity of some of the mobility indexes in these bistable regions (see Figures 1 and 2) and even seems to contradict the concept of a climatically determined index of dune mobility. This problem has been raised by Hugenholtz and Wolfe [2005], who gave as an example the juxtaposition of fully active dunes and relict stable dunes in the Kelso dune field, California. Lancaster [1994] suggested velocity amplification as a possible answer, but the phenomenon can also be explained by the fact that active and fixed dunes coexist under the same climatic conditions, as found by others [Muhs and Maat, 1993; Tsoar, 1995; Yizhaq *et al.*, 2007; Arens *et al.*, 2007]. Another problem with mobility indexes is that they take into account only current climatic parameters (e.g., precipitation, evapotranspiration and wind power). But dune response is known to lag behind climatic change [Hugenholtz and Wolfe, 2005]. For this reason, using changes in dune activity as an indicator of climate change is not decisive. The concept of dune mobility becomes even more complex when we have to consider vegetation cover as a stabilizing element. Because the rate of change of vegetation cover with climatic parameters (e.g., precipitation) is inherently nonlinear, dune dynamics is hysteretic in nature as shown in Figure 3.

[4] We recently suggested [Yizhaq *et al.*, 2007] a simple model for dune vegetation cover that exhibits dune bistability over a wide range of wind power regimes. Here, we generalize this dune dynamics model to include the effects of human activity (such as overgrazing, wood gathering and clear cutting) and precipitation. There is evidence for dune reactivation due to prolonged drought, for example, in the

<sup>1</sup>Department of Solar Energy and Environmental Physics, BIDR, Ben-Gurion University of the Negev, Midreshet Ben-Gurion, Israel.

<sup>2</sup>Department of Geography and Environmental Development, Ben-Gurion University of the Negev, Beer Sheva, Israel.

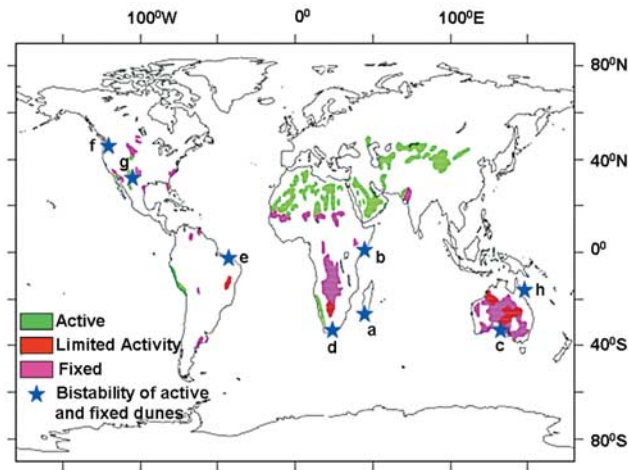


**Figure 1.** The global distribution of aeolian sand dunes according to mobility. The map follows *Thomas [1997]*, modified and supplemented with a few examples of locations where active and fixed dunes coexist. We emphasize that the map provides only a rough description of the location of the main sand seas.

northern Sinai [*Tsoar, 2005*] and southern Californian deserts [*Lancaster, 1997*]. On the basis of our model results, we suggest that, in some cases, once a sand dune becomes active (either because of increasing wind power, prolonged drought, or intense human activity), it will stay active even under the conditions under in which it was formerly fixed; in this situation, dune reactivation is an almost irreversible process.

[5] *Baas and Nield [2007]* and *Baas [2007]* have lately proposed a discrete (cellular automata) model of vegetated

dune landscape, in which the space is represented by a uniform grid of cells. The state of a given cell at a given (discrete) time is determined by a set of rules applied to the state of this cell and its neighbors at the previous time step. The advantages of such discrete models include their straightforward implementation, their low computational cost, and their ability to easily incorporate ecological and geomorphological aspects [*Fonstad, 2006*]. Alternatively, it is possible to model vegetation growth on sand dunes using continuum models [*Durán and Herrmann, 2006*] that describe the mean dynamics over scales that are larger than a single shrub but small enough relative to the system size to allow convenient calculations. Continuous models are, in most cases, more amenable to mathematical analysis than discrete models and are more favorable for dynamical analysis [*Guckenheimer and Holmes, 1983*]. The model presented here involves an implicit space equation expressed as an ordinary differential equation, a formulation that allows simple mathematical treatment.

**2. Model Formulation**

[6] Empirical studies have shown that dune activity can be modeled successfully using wind power and vegetation cover [*Hugenholtz and Wolfe, 2005*] as wind power determines sand transport capacity, while vegetation cover determines the amount of the sand available for transportation. This study seeks to model vegetation cover under the effect of wind, precipitation and human activity, and to relate dune mobility to different vegetation cover values. Recently, we developed a simple model that describes the growth of vegetation cover on sand dunes as a function of wind power [*Yizhaq et al., 2007*]. The model showed bistability and hysteresis with respect to wind power.

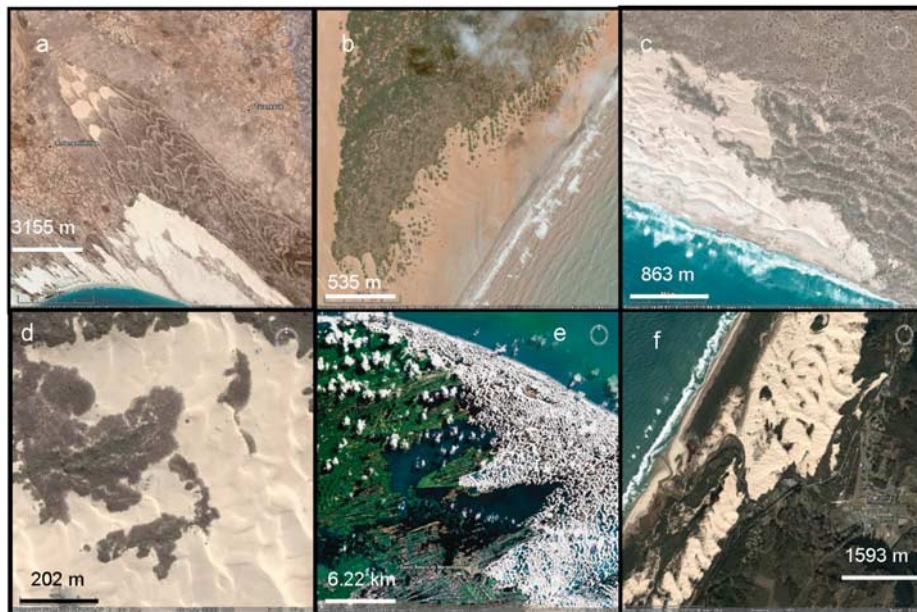


**Figure 2.** Areas in which active and fixed dunes coexist under similar climatic conditions “Google Earth imagery (© Google Inc., used with permission) containing imagery from TerraMetrics, Inc. (© 2009 TerraMetrics, Inc., <http://www.truearth.com>) and DigitalGlobe. The locations of the sites are indicated in Figure 1.

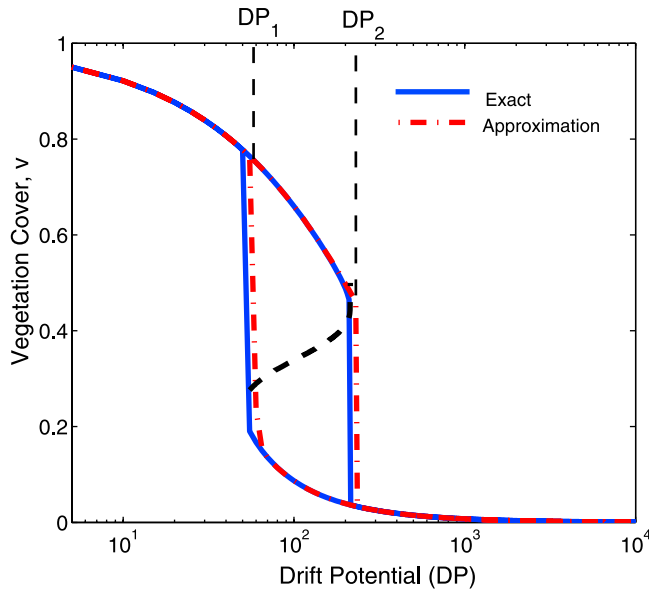


**Figure 3.** Stable states diagram showing the vegetation cover  $v$  versus DP for  $p = 80 \text{ mm a}^{-1}$ . The approximated solution (dash-dotted) is very close to exact numerical solution (solid). The unstable solution is marked with a dashed line. Parameter values used are  $v_{\max} = 1$ ,  $v_c = 0.3$ ,  $\epsilon = 0.001$ ,  $\gamma = 0.0008$ ,  $\eta = 0.2$ ,  $\mu = 0$ ,  $\alpha_{\max} = 0.15$ ,  $p_{\min} = 50 \text{ mm a}^{-1}$ ,  $c = 100$ , and  $b = 15$ .

Building on this early approach, the improved model we now propose is given as

$$\frac{dv}{dt} = \alpha(p)(v + \eta) \left(1 - \frac{v}{v_{\max}}\right) - \epsilon \text{DP} g(v_c, v)v - \gamma \text{DP}^{2/3} v - \mu v. \quad (1)$$

[7] Here,  $v$  is the dynamical variable representing areal vegetation cover density, which takes values between 0 (bare dune) and  $v_{\max} \leq 1$ . Vegetation dynamics is modeled using an implicit space logistic equation [Baudena et al., 2007] which assumes the area may be subdivided into neighboring sites that are vegetated or empty. The vegetation colonization rate,  $dv/dt$ , is represented by  $\alpha(p)(v + \eta)(1 - v/v_{\max})$ , a logistic growth function (growth  $\alpha(p)(v + \eta)$  times the competition term  $(1 - v/v_{\max})$ ).  $\eta$  is a spontaneous growth cover parameter that describes an average cover due to spontaneous growth for even bare dunes because of soil seed banks, underground roots, seeds carried by wind, animals, etc.  $v_{\max}$  denotes the maximum vegetation cover that the area can support, which depends on the type of vegetation and dune type.  $v_{\max}$  may also be associated with the vegetation carrying capacity of the system.

[8] In the model adopted here, we assume that the parameter  $\alpha$ , which denotes vegetative net growth, is a function of the annual precipitation ( $p$ ). Field studies [Bullard, 1997a] have shown positive relationships between precipitation and aboveground primary production, although the exact dependence is still unknown, especially for sand [Noy-Meir, 1973; Sala et al., 1988; Tsoar, 1996]. For larger amounts of rainfall the value of  $\alpha(p)$  becomes

saturated, as the amount of water that can be taken up by vegetation is limited. Moreover, since in our model  $\alpha(p)$  stands for an areal growth rate and not for biomass production, one expects maximal areal vegetation above a certain level of precipitation. Following observations, we assume that  $\alpha(p)$  converges to a maximum value  $\alpha_{\max}$  for sufficiently high precipitation rates [Tsoar, 2005]. On the other hand, we assume that vegetation cannot sustain itself below a minimal precipitation rate  $p_{\min}$ , as observed in extremely arid areas [Danin, 1996].  $p_{\min}$  may depend also on the potential evapotranspiration, but for simplicity we assume a constant value here. Without loss of generality, we can assume an exponential transition between these two limits. Thus,  $\alpha(p)$  may be expressed as

$$\alpha(p) = \begin{cases} \alpha_{\max}(1 - \exp(-(p - p_{\min})/c)) & p \geq p_{\min} \\ 0 & p < p_{\min} \end{cases} \quad (2)$$

The estimated value of  $p_{\min}$  is between  $50$  and  $80 \text{ mm a}^{-1}$  in the Nizzana (in the western Negev of Israel) area [Tsoar, 2005]; Danin [1996] similarly defined  $50 \text{ mm a}^{-1}$  as the threshold precipitation needed for perennial growth. We will therefore use  $p_{\min} = 50 \text{ mm a}^{-1}$  in the rest of this work.  $c$  quantifies the precipitation-dependent transition range between  $\alpha = 0$  and  $\alpha_{\max}$ : the smaller the value of  $c$ , the steeper the curve and the shorter the transition range is.  $c$  is related to the vegetative response to precipitation: larger values of  $c$  characterize shrubs, whereas smaller values are typical of herbaceous vegetation. The second term in equation (1),  $-\epsilon \text{DP} g(v_c, v)v$ , represents the effect of sand transport on vegetative growth, mainly due to root exposure and plant burial. We assume here that there is enough sand in the system which is available for wind transport. The effect of limited sand supply due to vegetation cover can be modeled by multiplying this term by  $(1 - v)$ , which is the exposed area. This correction has only a minor effect on the results presented in the current work. The vegetation cover also modifies the air flow pattern above the sand. Three types of air flow were previously identified according to the degree of vegetation cover, isolated roughness flow, wake interference flow, and skimming flow [Wolfe and Nickling, 1993]. In the isolated roughness and wake interference flows, the wind can act directly on the surface, whereas for skimming flow, while some amount of bare surface may be present, the sand is protected from the direct action of the wind by the surrounding vegetation. It was shown by Lee and Soliman [1977], who used wind tunnel experiments to investigate the densities of roughness elements, that a ground cover  $v_c$  of  $0.4$  provides sufficient blocking for skimming flow. This critical vegetation cover,  $v_c$ , further depends [Bullard, 1997a] on plant shape, porosity, stem flexibility, and wind velocity, as plant canopies can also be penetrated by strong winds. Thus, the interaction between vegetation and wind is quite complicated and nonlinear, making it difficult to estimate the value of  $v_c$ . Moreover,  $v_c$  varies for different geographical locations, from measured  $v_c \approx 0.14$ – $0.16$  for the Kalahari desert [Wiggs et al., 1995; Wiggs, 2008] to observed  $v_c \approx 0.35$  for the Australian deserts [Ash and Wasson, 1983].

[9] In our previous study [Yizhaq et al., 2007], we chose a step function for  $g(v_c, v)$ . However, it is more appropriate to choose a smoother transition function as it was noted

recently for the Simpson desert in Australia [Hesse and Simpson, 2006] that there is no simple vegetation cover threshold below which sand transport begins. Here we use a hyperbolic function for  $g(v_c, v)$

$$g(v_c, v) = 0.5(\tanh(b(v_c - v)) + 1), \quad (3)$$

where parameter  $b$  quantifies the steepness of the curve, the larger the value of  $b$ , the steeper is  $g(v_c, v)$ .  $b$  can be estimated from field and wind tunnel experiments. Note below that we also use a more simplified linear form for  $g(v_c, v)$  to enable analytical treatment.

[10] The DP term is a measure of wind power, usually expressed by aeolian geomorphologists as a drift potential (DP) [Fryberger, 1979; Tsoar, 2005], which is proportional to the potential sand volume that can be transported by the wind through a 1 m wide cross section per unit time (usually, it is given per year). DP is defined as

$$DP = \langle U^2(U - U_t) \rangle, \quad (4)$$

where  $U$  is the wind speed (in knots: 1 knot = 0.514 m s<sup>-1</sup>) measured at a height of 10 m and  $U_t$  is a minimal threshold velocity (= 12 knots) necessary for sand transport [Fryberger, 1979]. There are both theoretical and empirical linear relations between the drift potential and the rate of sand transport [Bullard, 1997b]. Still, the DP is a potential sand drift, as the actual drift further depends on the mean grain diameter, the degree of surface roughness, the amount and type of vegetation or crust cover, the amount of moisture in the sand, and the uniformity of wind direction. According to Fryberger [1979] wind energy can be classified into three classes: DP < 200, low energy; 200 ≤ DP < 400, intermediate energy; and DP ≥ 400, high energy. DP values in arid regions can vary from year to year (as does precipitation), as determined by the temporal activity pattern of storms. To avoid misconceptions, it should be understood that the DP in our model represents an average of several years and ignores the temporal variability.

[11] The parameter  $\varepsilon$  in equation (1) stands for the vegetation tolerance to sand erosion and deposition. As  $\varepsilon$  decreases, tolerance increases. In the model we do not distinguish between sand erosion and deposition, and the vegetation response is considered to depend on sand transport alone which is proportional to DP. It is also possible to include wind directionality in the model by replacing DP here with the resultant drift potential RDP, which is the resultant vector of DP values in each major wind direction (RDP ≤ DP); for simplicity, however, we prefer to keep the present form of the model.

[12] The third term in equation (1),  $\gamma DP^{2/3} v$  stands for a reduction in vegetation cover due to direct wind action, which increases evapotranspiration, as well as uproots, erodes, and suppresses vegetative growth [Hesp, 2002]. Generally, wind drag is proportional to the square of the wind speed [Bagnold, 1941], while DP is proportional to its cube. Thus DP<sup>2/3</sup> is used to represent wind drag on vegetation and thereby vegetative growth suppression due to direct wind action. This term is proportional to  $v$ , as it is

basically a mortality term. The parameter  $\gamma$  is a proportional constant that depends on vegetation types. It is important to note that, unlike the previous terms, this term acts even on maximally vegetated dunes.

[13] The last term in equation (1),  $-\mu v$ , stands for an extinction rate due to continuous human activity, as such grazing, clear cutting or burning. The intensity of this mortality term is governed by the value of the parameter  $\mu$  (negative values of  $\mu$  represent stabilization activities).

[14] It is possible to rewrite equation (1) in a simpler form with four parameters in the following form:

$$\frac{d\tilde{v}}{d\tau} = \alpha_1 \tilde{v} - \alpha_2 \tilde{v}^2 - \alpha_3 g(\tilde{v}_c, \tilde{v}) \tilde{v} + 1, \quad (5)$$

where the new parameters are defined as follows:  $\alpha_1 = (1 - \eta/v_{\max} - \gamma DP^{2/3} - \mu)/(\eta b)$ ,  $\alpha_2 = (\eta v_{\max} b^2)^{-1}$ ,  $\alpha_3 = -\varepsilon DP/(\alpha \eta b)$ ,  $\alpha_4 = b v_c$  and  $\tilde{v} = b v$ ,  $\tau = \alpha \eta b$ .  $\alpha_1$  is the new net vegetation growth rate,  $\alpha_2$  is a mortality term due to limited resources and  $\alpha_3$  is a mortality term due to sand transport. We prefer to keep the current form of equation (1) since it allows easier interpretation of the results.

[15] To obtain analytic solutions to the model in equation (1), it is useful to approximate  $g(v_c, v)$  (equation (3)) by the linear function  $f(v_c, v)$  as follows:

$$f(v_c, v) = \begin{cases} 1 & v < v_1 \\ \frac{1 + \tilde{b}(v_c - v)}{2} & v_1 \leq v \leq v_2 \\ 0 & v > v_2, \end{cases} \quad (6)$$

where we choose  $\tilde{b} = b/2.35$  with the 2.35 factor being an empirical factor chosen to fit the hyperbolic tangent function. Since for this value the linear approximation crosses the 99% (or 1%) value of the original function  $g(v_c, v)$ .  $v_{1,2}$  are given by

$$\begin{aligned} v_1 &= -1/\tilde{b} + v_c \\ v_2 &= 1/\tilde{b} + v_c \end{aligned} \quad (7)$$

The proposed model, i.e., equation (1), has two stable stationary states,  $A$  and  $F$ , representing active and fixed dunes, respectively. These solutions are

$$v_{a,f} = -\Gamma_{a,f} + \sqrt{\Gamma_{a,f}^2 + \eta v_{\max}}, \quad (8)$$

where

$$\begin{aligned} \Gamma_a &= \frac{v_{\max}}{2} \left( -1 + \eta/v_{\max} + \gamma DP^{2/3}/\alpha + \mu/\alpha \right) \\ \Gamma_f &= \frac{v_{\max}}{2} \left( -1 + \eta/v_{\max} + \gamma DP^{2/3}/\alpha + \mu/\alpha + \varepsilon DP/\alpha \right). \end{aligned} \quad (9)$$

[16] The active dune state  $v_a$  is valid for  $v < v_1$ , while the fixed dune state  $v_f$  is valid for  $v > v_2$ . For  $v_1 \leq v \leq v_2$  we used the linear approximation equation (6) to get the following expression for  $v_l$  which is the unstable solution:

$$v_l = -g_1 - \sqrt{g_1^2 + g_2}, \quad (10)$$

where

$$g_1 = \frac{v_{\max}}{2} \left( -1 + \eta/v_{\max} + \gamma DP^{2/3}/\alpha + \mu/\alpha - \varepsilon DP \tilde{b}/2\alpha \right)$$

$$g_2 = \frac{v_{\max}}{\alpha} [\alpha\eta - \varepsilon DP(1 + \tilde{b}v_c)/2]. \quad (11)$$

Figure 3 shows the stable stationary states as a function of DP for the exact and the approximate models; it can be seen that, indeed, the linear approximation for  $g(v_c, v)$  is quite good for the choice of parameters given in the Figure 3 caption.

[17] It is also possible to find the transition points from the active dune state to the fixed state (denoted by subscript 1 below) and from the fixed state to the active state (denoted by subscript 2 below) as follows. The fixed-active state transition occurs when  $v = v_2$  for a steady state condition  $dv/dt = 0$ . Using these two restrictions in equation (1) we obtain an equation for the fixed-active transition point:

$$\left( \gamma DP^{2/3} + \mu \right) v_2 = \alpha(p)(v_2 + \eta)(1 - v_2/v_{\max}), \quad (12)$$

where the transition can be found for any of the model's parameters. For example, when the control parameter is DP, the fixed-active dune transition is given by

$$DP_2^{2/3} = \alpha(v_2 + \eta)(1 - v_2/v_{\max})/(\gamma v_2) - \mu/\gamma. \quad (13)$$

Similarly, it is possible to find the fixed-active dune state transition points  $p_2$  and  $\mu_2$ .

[18] To estimate the transition from the active dune state to the fixed one we assume that the transition occurs at  $v = v_c$ . Similar to equation (12) we now obtain for the active-fixed transition

$$\left( \gamma DP^{2/3} + \varepsilon DP/2 + \mu \right) v_c = \alpha(p)(v_c + \eta)(1 - v_c/v_{\max}), \quad (14)$$

where the vegetation suppression due to sand transport is now also taken into account (via the  $\varepsilon$  term). Using this equation one may easily find the parameter values  $p_1$  and  $\mu_1$  at which the active-fixed transitions occur. The  $DP_1$  transition point is more difficult to evaluate, but it may be further approximated by

$$DP_1^{1/3} \approx (2\psi\gamma/\varepsilon)^{1/3} - 2\gamma/(3\varepsilon), \quad (15)$$

where  $\psi$  is given by

$$\psi = \alpha(v_c + \eta) \left( 1 - \frac{v_c}{v_{\max}} \right) / (\gamma v_c) - \mu/\gamma. \quad (16)$$

### 3. Results

[19] To further understand the model's solutions, we choose to use as control parameters, the wind drift potential DP, the annual precipitation  $p$ , and the human impact parameter  $\mu$ . The first two parameters may represent scenarios of climatic processes (i.e., windiness and rainfall) and the last describes anthropogenic activities, such as grazing

and clear cutting. Although the model has 9 parameters, it is possible to show that there are only 4 independent parameters; we prefer to apply the model using 9 parameters to allow easier interpretation of the model's results. Moreover, most of the parameters of the model can be estimated from previous works. For example concerning the spontaneous growth rate  $\eta$ , in a dune field in Nitzanim in Israel (located along the Mediterranean Sea), a vegetated dune was totally removed (including roots) and started to recover after a few years. The growth rate for bare ground and when no significant winds are present ( $DP = 0$ ) is  $\alpha\eta$  and thus  $\eta$  can be estimated as  $\Delta v/(\Delta t\alpha)$ . Thus, if for example, the vegetation cover after 1 year is 1.5%,  $\eta$  is  $0.015/1/0.1 = 0.15$ . This estimation is obviously rough and precise field experiments should be carried out in order to approximate this parameter for different plants and different dune types around the world.

[20] Similarly, a range of values can be estimated for the other parameters. Table 1 includes a range of values for each of the model's parameters, on the basis of the literature published on the subject. Except for the phenomenological parameters  $\varepsilon$  and  $\gamma$ , all the other parameters can be estimated. The range within which these two parameters fall can be indirectly found from the ranges of values of  $DP_1$  and  $DP_2$ , the transition points from the fixed to the active dune state and vice versa. The upper limit for  $DP_2$  can be estimated from the place with the highest DP value where the dunes are still fixed. Our estimation for this value is  $DP \sim 2000$ , but we overestimate it as 3000. An upper limit for  $DP_1$  is related to the location where only the fixed state exists but with lowest amount of rainfall. A reasonable approximation is  $DP_1 \approx 200$ . These arguments stand behind the range of values for  $\varepsilon$  and  $\gamma$  shown in Table 1. Direct estimations of these two parameters will require more careful and prolonged field or wind tunnel experiments.

[21] Figure 4 depicts the stationary solutions as a function of DP (Figure 4a),  $p$  (Figure 4b) and  $\mu$  (Figure 4c). Figure 4 shows hysteresis behavior, which means that the system responds differently to increasing or decreasing the control parameter from its extreme values, respectively. Each of these hysteresis diagrams can be interpreted as a desertification process, which is almost irreversible. For example, Figure 4a shows the model's response to changes in wind drift potential DP. For a wide range of DP values, both the fixed and active dune states coexist, indicating the hysteresis and bistability of the model. This dune behavior may be described as follows: starting from a very low DP, only the fixed dune solution  $v_f$  exists; when the DP slowly increases, this solution persists until the very high DP of  $DP_2$  is reached. Beyond this point, the system shifts into the active dune state,  $A$ . When DP is then slowly decreased, the solution continues to show active dune state until  $DP_1$  is reached, beyond which the solution reverts back to the fixed dune state. Note that, although the system has two stable solutions for the same parameters, a unique set of initial conditions determines only one possible final state. Only initial conditions that are scattered around the unstable branch can evolve to both final states. A large enough perturbation can switch the system from one stable state, across the unstable branch, to the other stable state. Several scenarios can lead to bistability of active and fixed dunes under the same climatic conditions. Among them are

**Table 1.** Definition and Typical Values of the Main Parameters Discussed in the Text

Parameter	Interpretation	Range	References
$\alpha_{\max}$	Maximum vegetation cover growth rate	0.1–0.2	<i>Hughenoltz and Wolfe</i> [2005]
$p_{\min}$	Minimal precipitation needed for vegetation growth	50 mm a <sup>-1</sup>	<i>Danin</i> [1996]
$c$	Vegetation growth response to precipitation	50–300 a <sup>-1</sup>	<i>Shmida et al.</i> [1986]
$\eta$	Spontaneous growth cover	0–0.2	<i>Arens et al.</i> [2007]
$v_{\max}$	Maximum vegetation cover	0–1	$v_{\max} = 1$ in the work by <i>Hughenoltz and Wolfe</i> [2005]
$v_c$	Critical vegetation cover	0.1–0.4	$v_c = 0.14$ in Kalahari dunes [ <i>Wiggs</i> , 2008], and $v_c = 0.35$ in Australian dunes [ <i>Ash and Wasson</i> , 1983], and $v_c = 0.17$ in Nizzana dunes [ <i>Allgaier</i> , 2008]
$b$	Steepness of transition between interference flow and skimming flow	5–20	<i>Ash and Wasson</i> [1983, Figure 1]
$\mu$	Human impact parameter	0–0.1	Can be estimated as 0.0008 for Sinai dunes between 1986 and 1989 [ <i>Meir and Tsoar</i> , 1996]
$\epsilon$	Vegetation tolerance to sand transport	0.005–0.02	Control the value of DP <sub>1</sub> DP <sub>1</sub> values are between 30 and 200
$\gamma$	Vegetation vulnerability to wind shear stress	0.005–0.02	Control the value of DP <sub>2</sub> 1500 ≤ DP <sub>2</sub> ≤ 3000

climate change and human impact. An example of such a transition is the clear cutting of vegetation on dunes in North Holland that took place in December 1998 (DP = 1706) [*Arens et al.*, 2007], which led to the dunes remaining bare and active until today.

[22] The behavior for  $p$  is obverse to that of DP, as increasing the value of  $p$  shifts the system into the fixed state, whereas decreasing  $p$  beyond a threshold value  $p_1$  shifts the system into the active state solution. The system's response to changes in the value of  $\mu$  is similar to that of DP, as increasing the value of  $\mu$  beyond  $\mu_2$  shifts the system from the fixed state to the active one.

[23] More important, even without climatic changes, overgrazing can shift the system from the fixed state to the active one. The opposite scenario is also possible; that is, stopping grazing can stabilize the dunes. This processes was observed at the coastal dunes of Ashdod-Nizana in Israel [*Levin and Ben-Dor*, 2004], where grazing and cutting practices of Bedouin between the late 1960s and the late 1970s led to dune activation and after these

practices were prohibited, the vegetation recovered and stabilized the dunes. Similar restabilization occurred in southern Israel, after the establishment of the Israel-Egypt border in 1982 [*Karnieli and Tsoar*, 1995].

[24] The typical timescales for convergence to the steady states can be found from the analytic solution of equation (1) for  $g(v_c, v) = 0$  and  $g(v_c, v) = 1$ , which can be written as

$$v(t) = (1/2\beta) \left( a - \sqrt{A} \tanh B \right), \quad (17)$$

where  $\beta = \alpha(p)/v_{\max}$ ,

$$a = \begin{cases} \alpha(p) - \alpha(p)\eta/v_{\max} - \epsilon DP - \gamma DP^{2/3} - \mu & v < v_c \\ \alpha(p) - \alpha(p)\eta/v_{\max} - \gamma DP^{2/3} - \mu & v \geq v_c, \end{cases} \quad (18)$$

and  $A = a^2 + 4bc_1$ , and  $c_1 = \alpha(p)\eta$ ;  $B = (\sqrt{A}/2)(C - t)$ , with  $C$  is an integration constant that depends on the initial condition. The characteristic convergence timescales as  $2/\sqrt{A}$ . Figure 5 shows the typical time  $\tau$  as a function of the

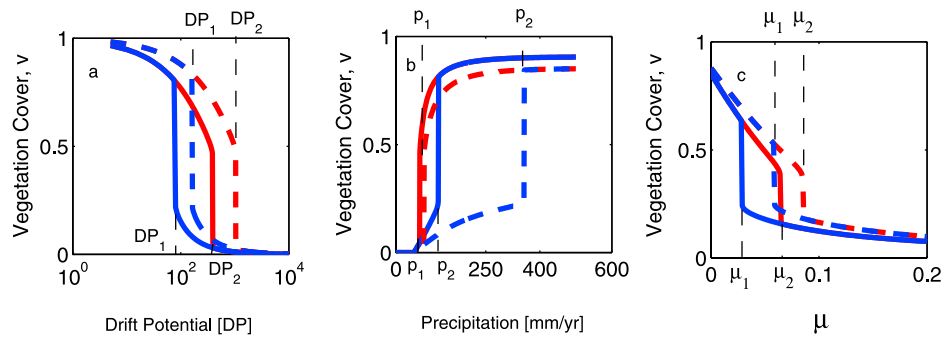


**Figure 4.** Stable states diagrams showing vegetation cover  $v$  versus DP, precipitation  $p$ , and  $\mu$ . (a) Vegetation cover versus DP for  $p = 100$  mm a<sup>-1</sup> (solid),  $p = 200$  mm a<sup>-1</sup> (dashed), and  $\mu = 0$ . (b) Vegetation cover versus  $p$  for DP = 200 (dashed), DP = 100 (solid), and  $\mu = 0$ . (c) Vegetation cover versus  $\mu$  for DP = 100,  $p = 150$  mm a<sup>-1</sup> (solid), and  $p = 200$  mm a<sup>-1</sup> (dashed). Parameter values used are  $v_{\max} = 1$ ,  $v_c = 0.3$ ,  $\epsilon = 0.001$ ,  $\gamma = 0.0008$ ,  $\eta = 0.2$ ,  $\alpha_{\max} = 0.15$ ,  $p_{\min} = 50$  mm a<sup>-1</sup>,  $c = 100$ , and  $b = 15$ .

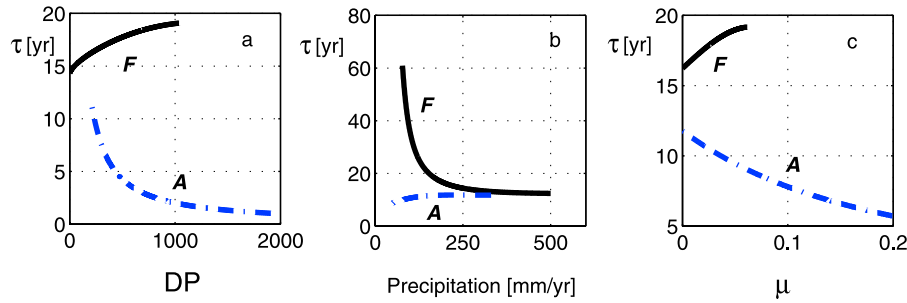


**Figure 5.** Typical convergence times  $\tau$  to the steady state solutions  $A$  (dash-dotted) and  $F$  (solid) as a function of the control parameters: (a) DP (for  $p = 200$  and  $\mu = 0$ ), (b) precipitation (for DP = 200 and  $\mu = 0$ ), and (c) human impact factor  $\mu$  (for DP =  $p = 200$ ). Values of the other parameters are as given in Figure 4.

control parameters DP,  $p$  and  $\mu$  for a domain where the solution (equation (17)) is valid. This characteristic time was termed by *Gaylord and Stetler* [1994] the aeolian response time, which depends on vegetation type. Figure 5 shows that the stabilization process is much slower than dune activation, especially for high values of DP. This asymmetry in the lengths of the activation time compared to the stabilization time is in accordance with field observations [*Hugenholtz and Wolfe*, 2005]. It is important to note that the stabilization process can be very fast in cases where

there is a biogenic crust as in the Nizzana dunes in the western Negev of Israel. In the current work we do not take into account the biogenic crust.

[25] The values of DP<sub>1</sub> and DP<sub>2</sub> as a function of precipitation rate,  $p$ , were computed numerically for different values of  $v_c$  and are shown in Figure 6. As  $v_c$  increases the fixed-active and active-fixed dune transitions occur for weaker winds (lower DP values). Above a certain value of precipitation (which depends on choice of parameters), the amount of rainfall is no longer the limiting factor [*Tsoar*,

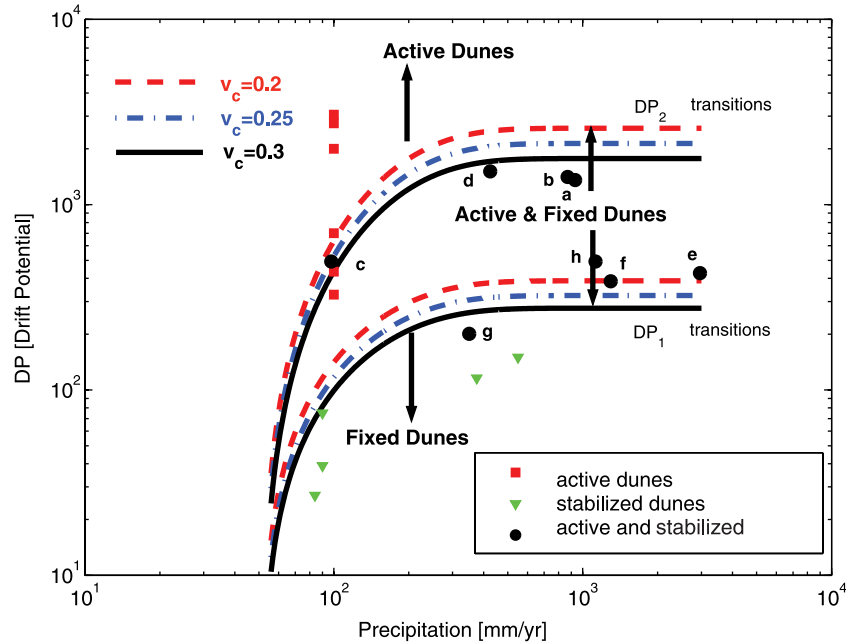


**Figure 6.** Numerical computation of the active-to-fixed dune transition point DP<sub>1</sub> and the fixed-to-active dune transition point DP<sub>2</sub> for different values of  $v_c$  as a function of precipitation rate  $p$ . In the regime below the DP<sub>1</sub> curves, dunes are fixed, whereas in the regime above the DP<sub>2</sub> curves, the dunes are active. In the intermediate regime, active and fixed dunes can coexist. Here  $\mu = 0$ , and the other parameters are as given in Figure 4. The labeled points indicate dune fields from different locations, which are marked according to their mobility (see the inset). The data were collected from the International Station Meteorological Climate Summary, version 3.0. The letters adjacent to the bistable dunes indicate dune locations given in Figure 1, and the precipitation values for these points are those of NCEP-NCAR reanalysis EAR40 database [*Kalnay et al.*, 1996]. The parameter values are within the ranges given in Table 1 and were further chosen to tune the data:  $v_{\max} = 1$ ,  $\epsilon = 0.001$ ,  $\gamma = 0.0008$ ,  $\eta = 0.2$ ,  $\alpha_{\max} = 0.15$ ,  $\mu = 0$ ,  $p_{\min} = 50 \text{ mm a}^{-1}$ ,  $c = 100$ , and  $b = 15$ .

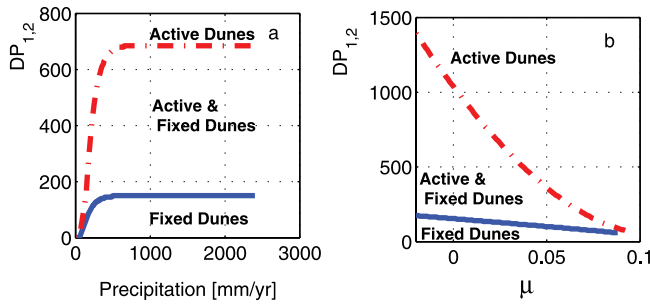


**Figure 7.** Active-to-fixed dune transition point  $DP_1$  (solid line) and fixed-to-active dune transition point  $DP_2$  (dash-dotted line) computed numerically by solving equation (1). (a)  $DP_1$  and  $DP_2$  as a function of precipitation. (b)  $DP_1$  and  $DP_2$  as a function of the human impact parameter  $\mu$ .

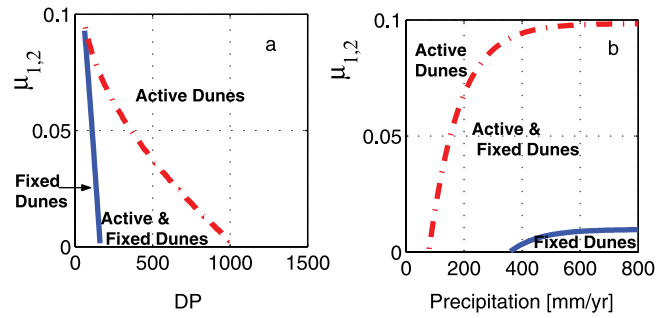


**Figure 9.** Active-to-fixed dune transition point  $\mu_1$  (solid line) and fixed-to-active dune transition point  $\mu_2$  (dash-dotted line) computed numerically by solving equation (1): (a)  $\mu_1$  and  $\mu_2$  as a function of the drift potential DP and (b)  $\mu_1$  and  $\mu_2$  as a function of precipitation  $p$ .

2005] and wind power takes over. Below this value ( $\sim 800 \text{ mm a}^{-1}$  for the present choice of parameters), the amount of rainfall is important for understanding dune dynamics as was observed in many studies that relate dune activity to dry conditions and ignore the wind effects [see, e.g., *Hugenholtz and Wolfe, 2005; Arens et al., 2004*]. Figure 6 shows that there is a good agreement between observations and model predictions using values within the limits given in Table 1. Thus, field observations can help to tune the parameters and partially validate the model's predictions.

[26] Almost all the bistable dune areas that we found are along coasts (see Figures 1 and 2). On one hand, the coexistence of active and fixed dunes requires relatively high precipitation to support vegetation growth, while on the other hand, coexistence requires high DP values to erode/bury vegetation, which maintains dune activity. Such areas are commonly found along coasts [*Hesp, 2004*]. In addition to strong wind power and high precipitation, a large sand supply is also necessary [*Arens et al., 2007*] for dune reactivation. The available sand comes either from the beach or from bare sand sheets and is controlled by vegetation cover [*Lancaster, 1999*]. In places with limited sand supply the dunes will eventually stabilize.

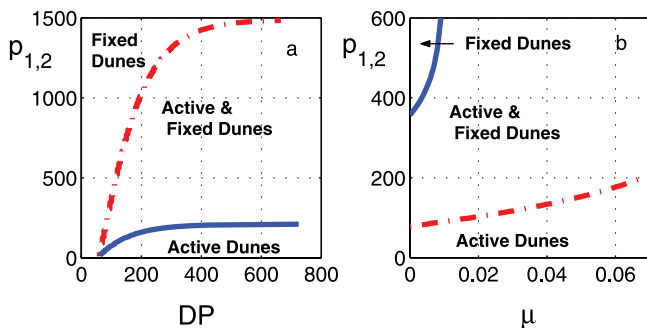


**Figure 8.** Active-to-fixed dune transition point  $p_1$  (solid line) and fixed-to-active dune transition point  $p_2$  (dash-dotted line) computed numerically by solving equation (1): (a)  $p_1$  and  $p_2$  as a function of the drift potential DP and (b)  $p_1$  and  $p_2$  as a function of the human impact parameter  $\mu$ .

[27] It is interesting to study the transition state wind power,  $DP_{1,2}$  as a function of precipitation (Figure 7a). For lower values of precipitation, the transition from the fixed to active dunes (i.e., desertification) occurs at lower values of DP. Thus, fixed vegetated dunes in more arid regions are more prone to reactivation as a consequence of strengthening of wind power than those in less arid localities.

[28] The response of dunes to three of the control parameters, DP,  $p$ , and  $\mu$ , which may be associated with climate change and human impact, are summarized in Figures 7, 8, and 9. Hysteretic behavior can be seen in the function of each of these parameters, but each graph depicts a different scenario. Figure 7 shows the active-to-fixed dune transition curve  $DP_1$  (blue line) and the fixed-to-active dune transition curve  $DP_2$  (red line), which are computed numerically by solving equation (1) as a function of precipitation  $p$  (Figure 7a) and  $\mu$  (Figure 7b). More rainfall (up to  $800 \text{ mm a}^{-1}$ ) means that more wind power is needed to shift dunes from the fixed to the mobile state, and vice versa. In contrast, increased  $\mu$  values, i.e., increased human impact, decreases the values of the transition points, especially  $DP_2$ , indicating that the system becomes more vulnerable for remobilization.

[29] In Figure 8, we show transition points  $p_{1,2}$  as a function of DP and  $\mu$ . It is clear from Figure 8a that the higher the value of DP, the higher the value of precipitation needed to trigger the transition. For example, in locales where wind power is great, the vegetative growth rate has also to be large in order to overcome wind erosion: higher values of  $p_2$  will support a larger growth rate. Figure 8b depicts  $p_{1,2}$  curves as a function of  $\mu$ . Note that the area above the  $p_1$  curve is very small; that is, for higher values of  $\mu$  only the active state is stable independent of precipitation rate.

[30] Figure 9 completes the description and shows the active-to-fixed dune transition point  $\mu_1$  (blue line) and fixed-to-active dune transition point  $\mu_2$  (red line) as a function of DP and  $p$ .  $\mu_1$  and  $\mu_2$  decrease monotonically for higher values of DP (Figure 9a) and behave in the obverse manner for increasing values of  $p$  (Figure 9b). This suggests that increased wind power enhances dune reactivation in the sense that even minor human activity may switch a fixed dune into the active state. The opposite happens for increased precipitation, namely when precipi-

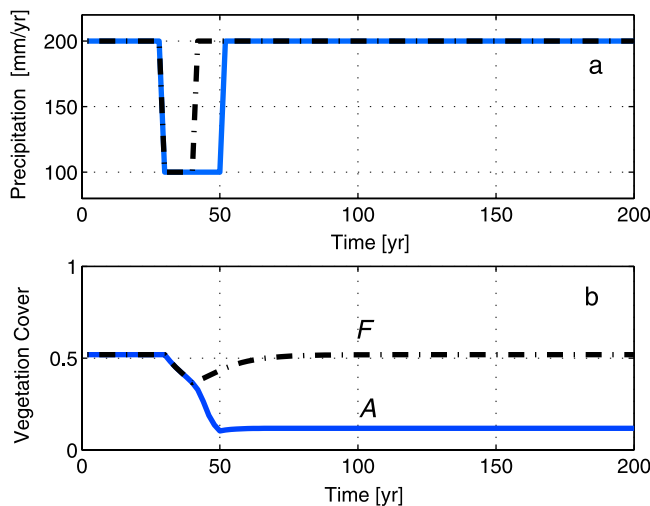


**Figure 10.** Vegetation response to prolonged droughts. (a) Two scenarios of precipitation sequences are mapped, one with a reduction of the rainfall from 200 to 100 mm a<sup>-1</sup> for a period of 10 years (dash-dotted) and the other for a period of 20 years (solid). (b) For each scenario in Figure 10a, the evolution of vegetation cover is presented. In the case of 10 years of drought (black curve), vegetation recovers and the fixed dune state returns. However, for a prolonged 20 year drought (blue curve), the dunes converge to the active state and remain there despite the return of precipitation to its initial value. Parameters: DP = 200 and other parameters are as in Figure 4.

tation increases, more massive human activity is needed for dune remobilization.

#### 4. Dune Remobilization Under Climate Change and Human Activity

[31] The model described above allows us to investigate the response of vegetation to climate change (such as prolonged drought) or human intervention. Figure 10 shows two drought scenarios that differ in duration. In the first, the vegetation cover recovers and returns to its initial state, whereas in the second the drought is long enough to allow the dunes to remain active despite precipitation returning to its original value. For the prolonged drought case, the vegetation cover is reduced and reaches the locus of attraction of the active dune state alone, and it therefore converges to this state. This scenario represents desertification, which is defined as an irreversible decrease in biological productivity induced by an environmental change, and is captured in the model, which demonstrates bistability ranges of active and fixed dune states. Transitions of this kind are often referred to in the ecology literature as "catastrophic regime shifts" [Rietkerk *et al.*, 2004; Solé, 2007]. In cases where the fixed state is the only stable state, the decline of vegetation cover will be continuous and will not involve sharp transitions.

[32] An additional scenario that we tested is the response of vegetation to periodic droughts. Figure 11 shows two such cases, one with a 4 year drought every 20 years and the other with an 8 year drought every 20 years. For the short-

duration drought, the dune system remains in the fixed state although the vegetation cover fluctuates; in this case the vegetation wasn't reduced sufficiently to enter the locus of attraction of the active dune state. For the longer-duration droughts, after a transient time, the system shifts to the active state after the vegetation is reduced sufficiently to enter the locus of attraction of the active dune state. During the transition, the vegetation shows growth phases in accordance with the high values of rainfall. Note that only in the third cycle of drought does the system converge to the active state. The time needed to displace the dune systems to another state by applying perturbation is termed the response time [Hugenholtz and Wolfe, 2005] and depends on values of the parameters.

[33] Another scenario for desertification due to grazing or clear cutting is illustrated in Figure 12. In the model, vegetation mortality (due to human activity) is represented by  $\mu$ . Increasing the value of  $\mu$  from 0.1 to 0.11 during a period of 10 years reactivates the dunes irreversibly. Grazing and wood gathering are major problems in many countries (e.g., Somalia), which can be even greater during droughts. Even small changes in vegetation mortality as a result of anthropogenic factors such as grazing, agricultural burning or off-road traffic can irreversibly shift sand dunes into the active state. An example of such human-induced desertification was reported by Khalaf and Al-Ajmi [1993] for the Kuwait Desert. By comparing satellite images from 1977 and 1989, it was clear that the southern limit of the mobile sand sheets had moved 35 km in a southeasterly direction. This resulted from deterioration of the vegetated

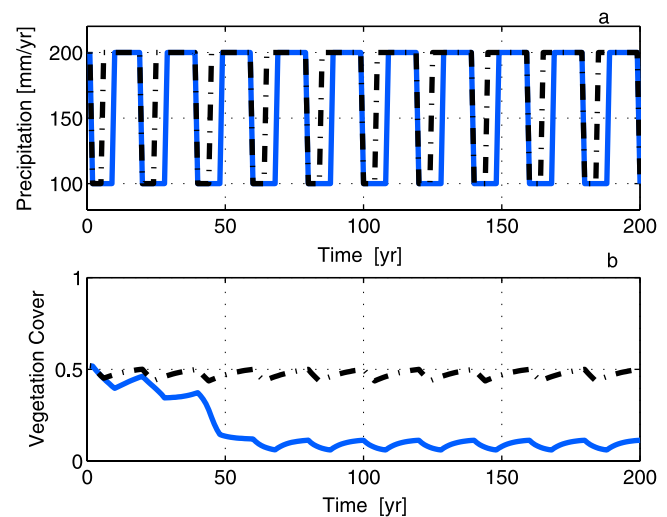


**Figure 11.** Vegetation response to periodic droughts. (a) Two scenarios of periodic precipitation sequences are presented, one with a reduction of the rainfall from 200 to 100 mm a<sup>-1</sup> over a period of 4 years (dash-dotted) and the other for a period of 8 years (solid) every 20 years. (b) For each scenario in Figure 11a, the evolution of vegetation cover with time is presented. For the shorter-duration droughts the vegetation cover remains in the fixed state with small fluctuations, while for the longer-duration droughts the vegetation cover drops to the active dune state and remains there. Parameters: DP = 200, with other parameters as given in Figure 4.

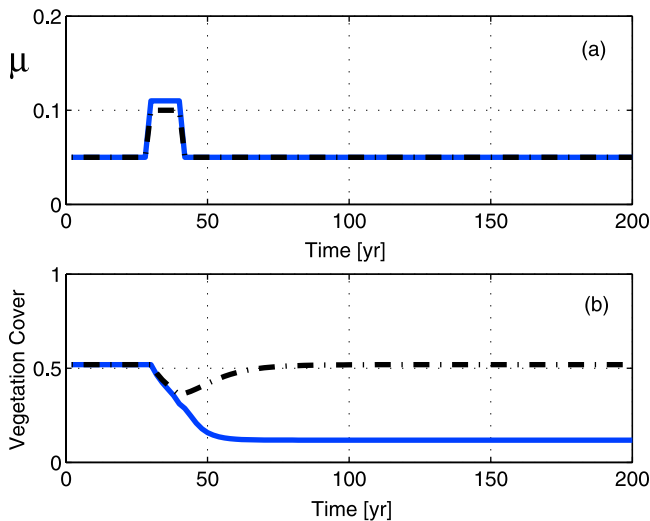


**Figure 12.** Vegetative response to grazing for the bistable case. (a) Two scenarios of overgrazing are represented with  $\mu$  going from 0.05 to 0.1 (dash-dotted) or to 0.11 (solid) for 10 years. (b) Vegetation cover time evolution in response to the overgrazing sequences in Figure 12a. After 10 years of grazing at  $\mu = 0.1$ , the vegetation recovered and returned to the fixed state, while for higher-intensity grazing at  $\mu = 0.11$  it converges to the active state and remains there even when the grazing returns to its initial value of  $\mu = 0.05$ . Parameters:  $DP = 200$ , with other parameters as given in Figure 4.

sand sheet due to human activities, which included overgrazing and woody shrub collecting. Our model shows that dunes or sand sheets may remain active even though human perturbation ceases.

## 5. Discussion

[34] The model we present here extends our previous work [Yizhaq *et al.*, 2007] in several ways: (1) Here we take into account the effect of precipitation on vegetation growth rates; that is,  $\alpha$  is a function of  $p$  and is not constant. (2) We replace the step function with a continuous function for the vegetation response to the sand transport term. (3) The current model also includes a grazing/clear cutting term. The above modifications allow us to use the model to explore different activation/stabilization scenarios under climatic changes as well as anthropogenic activities. The model can be used to investigate dune mobility in more informative ways than are available using indices of mobility regularly applied by aeolian geomorphologists.

[35] The proposed model can suggest possible scenarios for future dune mobility by using climatic data from GCM models. The main factor that affects dune mobility is wind power, though the amount of precipitation is also important for a certain range of values. First, there is the lower threshold of precipitation (taken as  $50 \text{ mm a}^{-1}$  in our simulations) which is necessary for vegetation growth. An upper threshold (taken as  $\sim 800 \text{ mm a}^{-1}$ ) also exists because above this point rainfall will not enhance vegetative cover, as groundwater has already reached its maximal capacity. Between these two thresholds the amount of precipitation

can affect dune mobility, and increased aridity can be related to higher dune mobility and vice versa. Prolonged droughts have a greater impact on dune reactivation when precipitation values are close to the lower threshold, i.e., in more arid environments.

[36] Our model also shows that mobile and fixed dunes can coexist under the same climatic conditions and that the processes of activation and stabilization are not symmetrical; once the stabilized dunes become active in response to climatic change or human intervention, much weaker wind power or much higher precipitation rates are required to restabilize the dunes. Therefore, as dune remobilization intensifies, steps such as reduced grazing and enhanced seeding [Wolfe *et al.*, 1997] must be taken to prevent vegetative cover decline from reaching its critical threshold. Once degradation reaches this state, reversal is difficult and costly. According to our model, prolonged droughts and increasing windiness due to climatic change, combined with grazing or clear cutting, may turn currently stable, vegetated dunes into mobile, bare dunes. From the point of view of dune management, it will be useful to identify the critical vegetation cover below which transition to the fully activated state occurs. Figure 4 can give some insight into how these critical values depend on the different model parameters.

[37] In the present model, we consider the interaction between vegetation, wind and sand, but in many dune fields the biogenic crust plays a crucial role in dune stabilization. Biogenic crusts are commonly found on sand dunes in the dry regions of the world (Africa, Australia, and Asia); they can resist long periods of drought and recover biological activity following rainfall [West, 1990; Benlap and Lange, 2001]. A continuous crust cover can withstand even the strongest wind intensities. By adding a second dynamic variable for the biogenic crust to our model, we will be able to reconstruct with greater accuracy the mutual interactions between crust, vegetation, wind and sand.

## 6. Conclusions

[38] The model presented here for vegetation cover dynamics of sand dunes takes wind power, precipitation and human pressure as its major variables. The model shows the coexistence of active and fixed dunes over a large range of drift potentials and precipitation values. Areas in which active and fixed dunes coexist are characterized by high values of  $DP$  and precipitation, in agreement with the model's prediction. The model shows that the transition from one model state to another can be irreversible and discontinuous in the bistability regime of active and fixed dunes.

[39] **Acknowledgments.** We thank the Israeli Ministry of the Environment and the Israel Science Foundation, grant 1122/07 for financial support. We thank Y. Zarmi and J. von Hardenberg for helpful discussions.

## References

- Alexander, W. (2007), Locally-developed climate model verified: Climate prediction, *Water Wheel*, 6(1), 27–29.
- Allgaier, A. (2008), Aeolian sand transport and vegetation cover, in *Arid Dunes Ecosystems*, edited by S.-W. Breckle, A. Yair, and M. Veste, pp. 211–224, Springer, Berlin.
- Andreotti, B., P. Claudin, and S. Douady (2002), Selection of dune shapes and velocities, part 2: A two-dimensional modelling, *Eur. Phys. J. B*, 28, 341–352.

- Arens, S. M., Q. Slings, and C. N. de Vries (2004), Mobility of a remobilised parabolic dune in Kennemerland, the Netherlands, *Geomorphology*, *59*, 175–188.
- Arens, S. M., Q. Slings, L. Geelen, and H. Van der Hagen (2007), Implications of environmental change for dune mobility in the Netherlands, paper presented at International Conference on Management and Restoration of Coastal Dunes, Minist. de Medio Ambiente, Santander, Spain, 3–5 Oct.
- Ash, J. E., and R. J. Wasson (1983), Vegetation and sand mobility in the Australian desert dunefield, *Z. Geomorphol.*, *45*, 7–25.
- Baas, A. C. W. (2007), Complex systems in aeolian geomorphology, *Geomorphology*, *91*, 311–331.
- Baas, A. C. W., and J. M. Nield (2007), Modelling vegetated dune landscapes, *Geophys. Res. Lett.*, *34*, L06405, doi:10.1029/2006GL029152.
- Bagnold, R. A. (1941), *The Physics of Blown Sands and Desert Dunes*, Chapman and Hall, London.
- Baudena, M., G. Boni, L. Ferraris, J. von Hardenberg, and A. Provenzale (2007), Vegetation response to rainfall intermittency in drylands: Results from a simple ecohydrological box model, *Adv. Water Resour.*, *30*, 1320–1328.
- Benlap, J., and O. L. Lange (2001), *Biological Soil Crusts: Structure, Function, and Management*, Springer, Berlin.
- Bullard, J. (1997a), Vegetation and dryland geomorphology, in *Arid Zone Geomorphology*, edited by D. S. G. Thomas, chap. 7, pp. 109–131, John Wiley, Chichester, U.K.
- Bullard, J. E. (1997b), A note on the use of the “Fryberger method” for evaluating potential sand transport by wind, *J. Sediment. Res.*, *67*(3), 499–501.
- Danin, A. (1996), *Plants of Desert Dunes*, Springer, Berlin.
- Dong, Z., G. Chen, X. He, Z. Han, and X. Wang (2005), Controlling blown sand along the highway crossing the Taklimakan Desert, *J. Arid Environ.*, *57*, 329–344.
- Durán, O., and H. J. Herrmann (2006), Vegetation against dune mobility, *Phys. Rev. Lett.*, *97*, 188001.
- Fonstad, M. A. (2006), Cellular automata as analysis and synthesis engines at the geomorphology-ecology interface, *Geomorphology*, *77*, 217–234.
- Fryberger, S. G. (1979), Dune forms and wind regime, in *A Study of Global Sand Seas*, edited by E. D. McKee, *U.S. Geol. Surv. Prof. Pap.*, *1052*, 137–169.
- Gaylord, D. R., and L. D. Stetler (1994), Aeolian-climatic thresholds and sand dunes at the Hanford site, south-central Washington, USA, *J. Arid Environ.*, *28*, 95–116.
- Guckenheimer, J., and P. Holmes (1983), *Nonlinear Oscillations, Dynamical Systems and Bifurcations of Vector Fields*, Springer, New York.
- Herrmann, H. J. (2006), Pattern formation of dunes, *Nonlinear Dyn.*, *44*, 315–327.
- Hesp, P. (2002), Foredunes and blowouts: Initiation, geomorphology and dynamics, *Geomorphology*, *48*, 245–268.
- Hesp, P. A. (2004), Coastal dunes in the tropics and temperate regions: Location, formation, morphology and vegetation processes, in *Coastal Dunes: Ecology and Conservation*, edited by M. L. Martínez and N. P. Psuty, pp. 29–49, Springer, Berlin.
- Hesse, P. P., and R. L. Simpson (2006), Variable vegetation cover and episodic sand movement on longitudinal desert sand dunes, *Geomorphology*, *81*, 276–291.
- Hugenholtz, C. H., and S. A. Wolfe (2005), Biogeomorphic model of dunefield activation and stabilization on the northern Great Plains, *Geomorphology*, *70*, 53–70.
- Kalnay, E., et al. (1996), The NCEP/NCAR 40-year reanalysis project, *Bull. Am. Meteorol. Soc.*, *77*(3), 437–471.
- Karnieli, A., and H. Tsoar (1995), Spectral reflectance of biogenic crust developed on desert dune sand along the Israel-Egypt border, *Int. J. Remote Sens.*, *16*(2), 369–374.
- Khalaf, M., and D. Al-Ajmi (1993), Aeolian processes and sand encroachment problems in Kuwait, *Geomorphology*, *6*, 111–134.
- Knight, M., D. S. G. Thomas, and G. F. S. Wiggs (2004), Challenges of calculating dunefield mobility over the 21st century, *Geomorphology*, *59*, 197–213.
- Lancaster, N. (1994), Controls on aeolian activity: New perspectives from Kelso dunes, Mojave Desert, California, *J. Arid Environ.*, *27*, 113–124.
- Lancaster, N. (1997), Response of eolian geomorphic systems to minor climate change: Examples from the southern Californian deserts, *Geomorphology*, *19*, 333–347.
- Lancaster, N. (1999), Geomorphology of desert sand seas, in *Aeolian Environments, Sediments and Landforms*, edited by A. S. Goudie, I. Livingstone, and S. Stokes, pp. 49–69, John Wiley, Chichester, U.K.
- Lee, B. E., and B. F. Soliman (1977), An investigation of the forces on three dimensional bluff bodies in rough wall turbulent boundary layers, *J. Fluids Eng.*, *99*(3), 503–510.
- Levin, N., and E. Ben-Dor (2004), Monitoring the dune stabilization process along the coastal dunes of Ashdod-Nizanim, Israel, 1945–1999, *J. Arid Environ.*, *58*, 335–355.
- Meir, A., and H. Tsoar (1996), International borders and range ecology: The case of Bedouin transborder grazing, *Hum. Ecol.*, *24*(1), 39–64.
- Muhs, D. R., and P. B. Maat (1993), The potential response of eolian sands to greenhouse warming and precipitation reduction on the Great Plains of the U.S.A., *J. Arid Environ.*, *25*, 351–361.
- Noy-Meir, I. (1973), Desert ecosystems: Environment and producers, *Annu. Rev. Ecol. Syst.*, *4*, 25–51.
- Pye, K., and H. Tsoar (1990), *Aeolian Sand and Sand Dunes*, Unwin Hyman, London.
- Rietkerk, M., S. C. Dekker, P. C. de Ruiter, and J. van de Koppel (2004), Self-organized patchiness and catastrophic shifts in ecosystems, *Science*, *305*, 1926–1929.
- Sala, O. E., W. J. Parton, L. A. Joyce, and W. K. Lauenroth (1988), Primary production of the central grassland region of the United States, *Ecology*, *69*(1), 40–45.
- Shmida, A., M. Evenari, and I. Noy-Meir (1986), Hot desert ecosystems: An integrated view, in *Hot Deserts and Arid Shrublands, Ecosyst. World*, vol. 12, edited by M. Evenari, I. Noy-Meir, and D. W. Goodall, pp. 379–387, Elsevier, Amsterdam.
- Solé, R. (2007), Scaling laws in the drier, *Nature*, *449*, 151–153.
- Thomas, D. S. G. (1997), Sand seas and aeolian bedforms, in *Arid Zone Geomorphology*, 2nd ed., edited by D. S. G. Thomas, chap. 17, pp. 373–412, John Wiley, New York.
- Thomas, D. S. G., M. Knight, and G. F. S. Wiggs (2005), Remobilization of southern African desert dune systems by twenty-first century global warming, *Nature*, *435*, 1218–1221.
- Tsoar, H. (1995), Desertification in northern Sinai in the eighteenth century, *Clim. Change*, *29*, 429–438.
- Tsoar, H. (1996), The effect of soil texture on the biomass in an arid region, in *The Mosaic of Israeli Geography*, edited by Y. Gradus and G. Lipshitz, pp. 385–391, Ben-Gurion Univ. of the Negev Press, Beer Sheva, Israel.
- Tsoar, H. (2005), Sand dunes mobility and stability in relation to climate, *Physica A*, *357*(1), 50–56.
- West, N. E. (1990), Structure and function of microphytic soil crusts in woodland ecosystems of arid to semi-arid regions, *Adv. Ecol. Res.*, *20*, 179–223.
- Wiggs, G. F. S. (2001), Desert dune processes and dynamics, *Prog. Phys. Geogr.*, *25*, 53–79.
- Wiggs, G. F. S. (2008), The non-linear response of aeolian sand dunes to changing climatic conditions and vegetation cover, *Geophys. Res. Abstr.*, *10*, abstract EGU2008-A-11757.
- Wiggs, G. F. S., I. Livingstone, D. S. G. Thomas, and J. E. Bullard (1995), Dune mobility and vegetation cover in the southwest Kalahari Desert, *Earth Surf. Processes Landforms*, *20*, 515–530.
- Wolfe, G., M. Steinke, and G. Kirst (1997), Grazing-activated chemical defence in a unicellular marine alga, *Nature*, *387*, 894–897.
- Wolfe, S. A., and W. C. Nickling (1993), The protective role of sparse vegetation in wind erosion, *Prog. Phys. Geogr.*, *17*, 50–68.
- Yizhaq, H., Y. Ashkenazy, and H. Tsoar (2007), Why do active and stabilized dunes coexist under the same climatic conditions?, *Phys. Rev. Lett.*, *98*, 188001.

Y. Ashkenazy and H. Yizhaq, Department of Solar Energy and Environmental Physics, BIDR, Ben-Gurion University of the Negev, Midreshet Ben-Gurion 84990, Israel. (yiyeh@bgu.ac.il)

H. Tsoar, Department of Geography and Environmental Development, Ben-Gurion University of the Negev, Beer Sheva 84105, Israel.